Hovering and Forward Flight Control of a Ducted Fan Unmanned Aerial Vehicle Based on PID Control

Mohammad Saleh Ahmadi
Dept. of Mechanical Eng.
Isfahan Univ. of Tech.
Isfahan, Iran
ms.ahmadipooladianar@me.iut.ac.ir

Hamid Hajkarami
Dept. of Mechanical Eng.
Isfahan Univ. of Tech.
Isfahan, Iran
h.hajkarami@me.iut.ac.ir

Afshin Manouchehri
Dept. of Mechanical Eng.
Kh. Sh. Azad Univ.
KhomeiniShahr, Iran
afhshin.manouchehri@gmail.com

***Abstract*—In this paper, the problem of hovering and forward flight control of a ducted fan Unmanned Aerial Vehicle (UAV) is addressed. For this purpose, a short review of the mechanical characteristics of the vehicle and also its mathematical model is presented. After that a two loop PID controller is constructed for both hovering and forward flight conditions. At the end, Numerical simulations are used to illustrate the performance of the developed controllers in certain and uncertain conditions.**

Keywords: Unmanned Aerial Vehicles (UAV), ducted fan, hovering control, forward flight control, PID control

I. INTRODUCTION

Recently, as the technology of UAV is evolved rapidly, the interest in the UAV has increased in military as well as civil applications. UAV can move easily to places where a man cannot approach in the war or emergency situations, so that the risk of the human participation can be reduced. Specially, the vertical take-off /landing (VTOL) crafts have more interest than the existing fixed-wing UAV because VTOL does not need a runway and can hover, and take-off vertically. In this paper, a ducted fan UAV among the VTOL has the spotlight due to compact design and various activities.

Because of the highly nonlinear characteristics of the dynamic equations of motion of the craft, previous works addressed the control problem of this type of UAVs with nonlinear control strategies [1, 2]. In this paper, in spite of its complicated and highly nonlinear equations of motion, a PID controller designed for hovering and forward flight maneuvers. The proposed controller is able to control the craft in the presence of different type of system uncertainties.

This paper is organized as follows. Section II briefly introduces the mechanical structure of the ducted fan aerial robot. The dynamic model of the craft is presented in section III, The PID controller is described in section IV, Computer simulations are shown in Section V and finally, section VI draws the main conclusions of this work.

II. MECHANICAL STRUCTURE OF THE DUCTED FAN UAV

A schematic view of a ducted fan prototype is shown in figure 1. As it is obvious in the figure, this vehicle is composed of a main duct, driving engine, propeller, anti torque and control rudders and landing legs. Increasing motor speed, we can increase the trust and adjust the vehicle altitude. Under the propeller, there are two levels of rudders with different structures. The first level rudders which rotate altogether but binary converse neutralize the motor torque. The second level rudders which are placed under the first level ones and outside the duct rotate together in the same direction to control the vehicle in the $x-y$ plane.

The major difference between ducted fan and other UAVs are a strong coupling effect and existence of a duct surrounding the rotor. When ducted fan UAV hovers, the vehicle is very unstable because of a strong coupling effect. Existence of a duct has some advantages for the vehicle. First of all, a duct guarantees safety more than any rotorcraft without a duct. The unshrouded propeller operating with high speed can do damage to somebody directly. On the other hand, if the craft bump into anything while it is operating, it can be damaged seriously by breaking the rotor. Secondly, a duct produces more efficient thrust with same power. The thrust of a craft with a duct is increased approximately 21% comparing with a ductless craft [3]. The unshrouded propeller has tip loss by escaping tip vortex at the blade tip. It results in rapid decrease in the lift at the tip. In addition, the duct tends to prevent air at the tip from escaping so that more thrust efficiency could be generated by lower energy loss. As a disadvantage of a duct, there are momentum drag and righting torque that disturb the forward flight at higher speeds [3]. As the craft forces the incoming flow in the duct to align it to downward, a reaction force is created, known as momentum drag. This force is same the mass flow of the air flow added crosswind velocity.

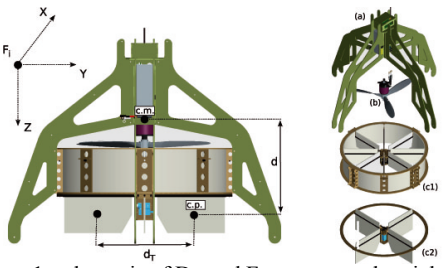

Figure 1. schematic of Ducted Fan unmanned aerial robot

III. DYNAMIC MODEL OF THE VEHICLE

in this section, the mathematical model of the ducted fan UAV is presented. using the Newton Euler equations, the ducted fan model can be described as [4]:

$$\begin{aligned} X - mgS_\theta &= m(\dot{u} + qw - rv) \\ Y + mgC_\theta S_\phi &= m(\dot{v} + ru - pw) \\ Z + mgC_\theta C_\phi &= m(\dot{w} + pv - qu) \end{aligned} \tag{1}$$

$$\begin{aligned} L &= I_x\dot{p} - I_{xx}\dot{r} + qr(I_z - I_y) - I_{xx}pq \\ M &= I_y\dot{q} + rp(I_x - I_z) + I_{xz}(p^2 - r^2) \\ N &= -I_{xz}\dot{p} + I_z\dot{r} + pq(I_y - I_x) + I_{xz}qr \end{aligned} \tag{2}$$

$$\begin{aligned} p &= \dot{\phi} - \dot{\psi}S_\theta \\ q &= \dot{\theta}C_\phi + \dot{\psi}C_\theta S_\phi \\ r &= \dot{\psi}C_\theta C_\phi - \dot{\theta}S_\phi \end{aligned} \tag{3}$$

$$\begin{aligned} \dot{\theta} &= qC\phi - rS_\phi \\ \dot{\phi} &= p + qS_\phi T_\theta + rC_\phi T_\theta \\ \dot{\psi} &= (qS_\phi + rC_\phi)(\frac{1}{C_\theta}) \end{aligned} \tag{4}$$

where m represent the vehicle mass, g the gravity, *X*, *Y* and *Z* forces exerted to the vehicle *L*, *M* and *N* torques to the vehicle, *u*, *v* and *w* linear velocities and *p*, *q* and *r* angular velocities of the vehicle respectively in the body attached frame. ϕ, θ and ψ are respectively roll, pitch and yaw angles of the ducted fan. S_x and C_x respectively stand for $\sin x$ and $\cos x$. The external forces to the UAV are as below:

$$\begin{aligned} X &= \rho c_L S^{l2}\alpha_x V_e^2 \\ Y &= \rho c_L S^{l2}\alpha_y V_e^2 \\ Z &= T - \rho c_D(2S^{l1} + 4S^{l2})V_e^2 + \rho(c_D S^{l2}(\alpha_x + \alpha_y) + 4c_D S^{l1}\alpha)V_e^2 \end{aligned} \tag{5}$$

In these equations, ρ is air density, c_L lift coefficient, c_D drag coefficient, α angle of attack of first level (anti torque) rudders, α_x and α_y the angle of attack of second level (control) rudders respectively in x and y directions, T the motor trust and S^{l1} and S^{l2} respectively are area of each of the first and second rudders. V_e is the exiting wind velocity from the bottom of the duct which can be calculated as:

$$V_e = \sqrt{\frac{2T}{\rho S_{disk}}} \tag{6}$$

In which S_{disk} represent the cross section area of the duct. Like the external forces, the external torques can be classified as:

$$\begin{aligned} L &= -Xd \\ M &= Yd \\ N &= 4c_L(S^{l1}/S_{disk})d_T T\alpha + k_N\omega_P^2 \end{aligned} \tag{7}$$

Where d and d_T respectively are the distance from pressure center of the second level rudders to the vehicle center of mass and the distance between pressure center of each of two contrary control rudders(see figure 1). ω_p is the angular velocity of the propeller and k_N is a constant coefficient. It is noteworthy to say that in these equations, the drag force caused by horizontal motion of the vehicle, wind forces, drag forces of the rudders and also momentum drag of the duct are assumed to be zero. These assumptions are sufficiently correct for indoor hovering flights of the ducted fan UAV [5, 6].

IV. CONTROLLER

In spite of their simplicity, PID controllers have a good performance in many cases. The only problem (disadvantage) of these controllers to be used in large systems is that a big quantity of controllers is needed to cover the whole system [7]. All of these controllers have to be adjusted so that the maximum performance will be obtained. Instead, these types of controllers are easy to implement and regulate. In this research, two internal and external PID controllers are used. The block diagram of the internal and external loops is depicted in figure 2.

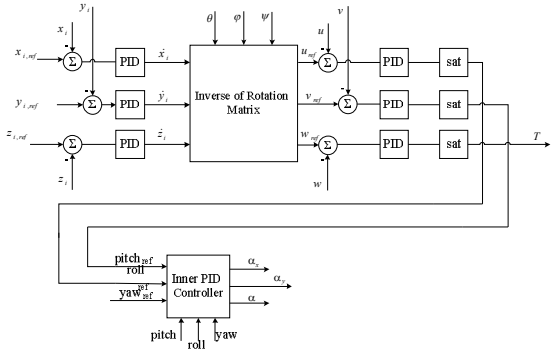

Figure 2. Block Diagram of proposed Controller

As it is clear in this figure, the desired values of x, y and z are given to the controller. For hovering maneuvers, the desired values of longitudinal and lateral position of the UAV (i. g. x_{des} and y_{des}) must be considered equal to zero. Using actual position of the UAV in space, the desired values of velocities in the inertia frame are calculated. Knowing Euler angles of the robot and using a rotation matrix, these

velocities are transformed to the desired velocities explained in the body attached frame. These values are compared with the actual velocities of the robot and will transform to the desired Euler angles (which cause the robot to go to the desired position) by three PID controllers. Since the lift can be calculated directly from the desired altitude and the robot horizontal velocity, we can extract the required trust here. The desired Euler angles passing through saturation functions (which simulate actual limitation of rudders rotation range) are given to the inner PID controller as the inputs. This controller calculates the appropriate angles of attack of first and second level rudders using the actual Euler angle of the robot. These angles in addition to the trust (which is calculated in the outer loop controller), are used as the inputs of the ducted fan system [8].

V. SIMULATION RESULTS

In this section, the performance of the proposed controller is simulated for an existing ducted fan. Numeric values of the ducted fan parameters are given in table 1. Computer simulations have been carried out using SIMULINK™ and MATLAB™ toolboxes. Because of brevity, only the forward flight simulations are presented. The goal is to send the robot to the point $A = (10, 2, 20)$, stay 10 seconds and then to the point $B = (0, 2, 4)$.

TABLE I. NUMERIC VALUES OF THE DUCTED FAN PARAMETERS

Parameter	Numeric Value
m	$1.576\ kg$
$\mathbf{I}$	$\begin{bmatrix} 0.018 & 0 & 0 \\ 0 & 0.018 & 0 \\ 0 & 0 & 0.009 \end{bmatrix} kgm^2$
I_{rot}	$0.0003 kgm^2$
d	$0.2075\ m$
d_T	$0.16\ m$
S^{l1}	$0.0073\ m^2$
S^{l2}	$0.0096\ m^2$
S_{disk}	$0.2\ m^2$

Figure 3 shows the vehicle actual and desired path in the 3D space. The angle of attack of anti torque and control rudders are plotted in figures 4, 5 and 6 respectively. Figure 7 depicts the trust. The maximum trust of the robot is limited to 20 N. According to these figures, it is clear that the robot has reached to the points A and B approximately within 10 seconds.

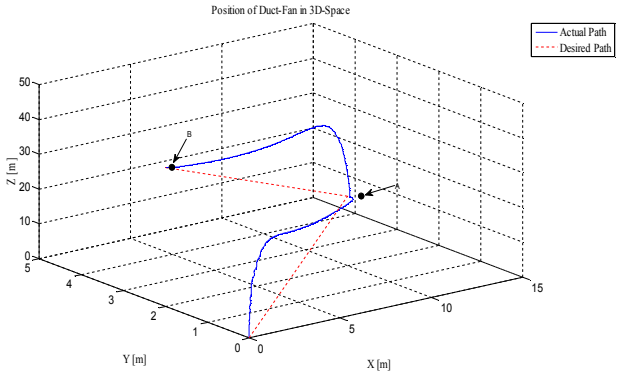

Figure 3. Ducted Fan actual and desired position

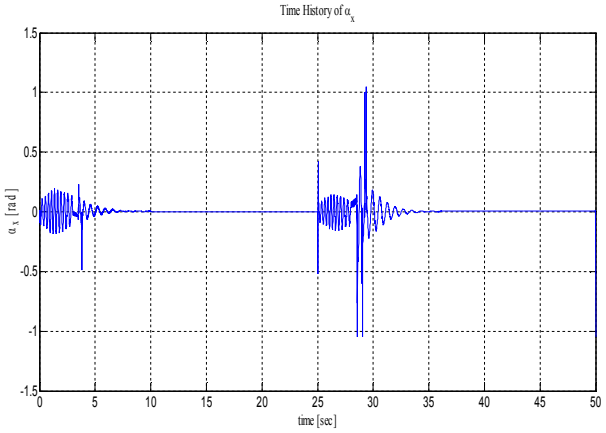

Figure 4. Angle of attack of control rudders in x direction

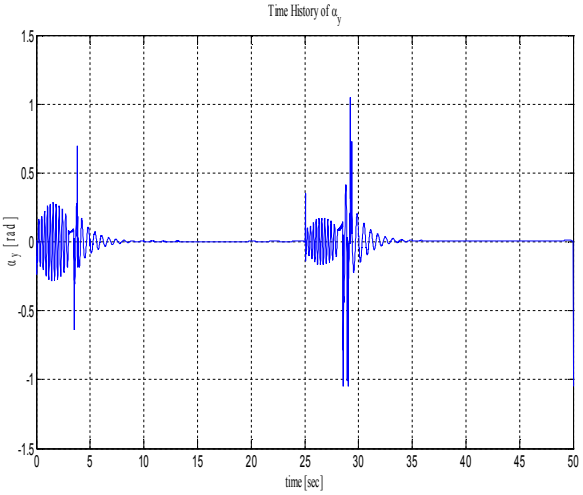

Figure 5.Angle of attack of control rudders in y direction

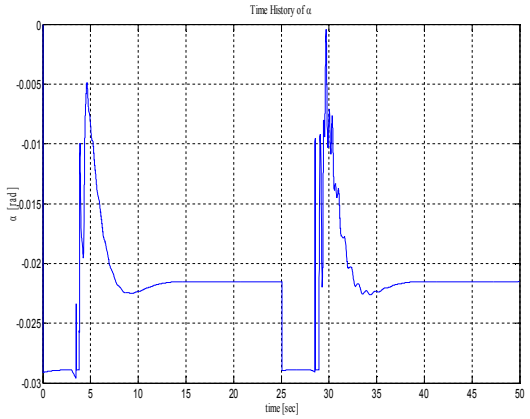

Figure 6. Angle of attack of anti torque rudders

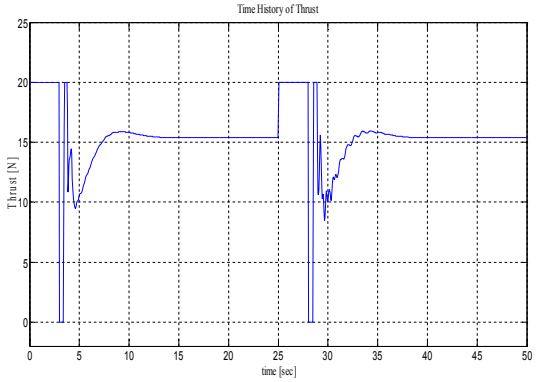

Figure 7. Trust

To show the robustness of the controller against parametric uncertainties, all of simulations were repeated considering twenty percent uncertainty in the robot parameters. Simulation results reveal good performance of controller facing uncertainties. For the sake of brevity, only robot altitude and trust for hovering flights considering 20% added mass are presented in figures 8 and 9 respectively. The goal is to send the robot to point $A = (0,0,20)$.

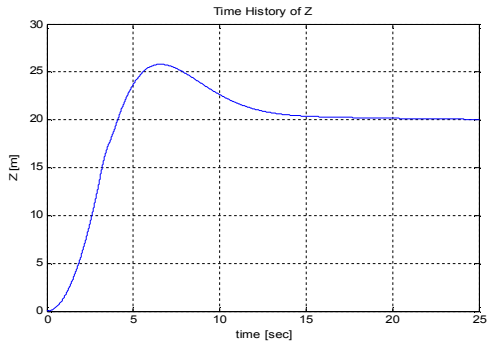

Figure 8. Ducted fan altitude considering 20% uncertainty in the mass of the ducted fan

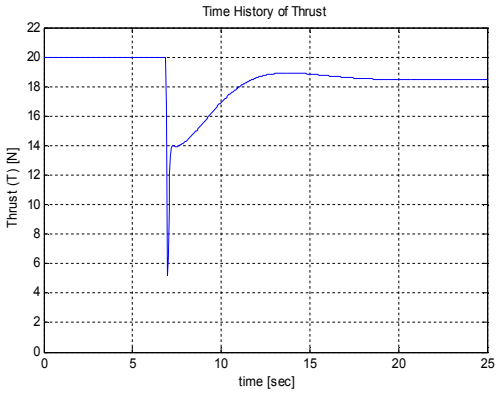

Figure 9. Trust considering 20% uncertainty in the mass of the ducted fan

VI. CONLUSIONS

In this research firstly the mathematical model of the ducted fan UAV is extracted and then a two loop PID controller is designed and regulated for hovering flight maneuvers. Numerical simulations are used to demonstrate the performance of the proposed controller. These results demonstrate the good performance of the designed controller. They also reveal the ability of the controller to withstand more than 20 percent uncertainty in system parameters.

REFERENCES

[1] Comparison of nonlinear control design techniques on a model of the Caltech ducted fan, Jie Yu, Ali Jadbabaie, James Primbs, Yun Huang, 2001, automatica

[2] Olfati-Saber, ‘‘Global configuration stabilization for the vtol aircraft with strong input coupling’’, IEEE Trans. Automat. Contr., 47, pp. 1949–1952, 2002a.

[3] Jonathan Fleming and Troy Jones, “Improving control system effectiveness for ducted fan VTOL UAVs operating in crosswinds,” 2nd AIAA “Unmanned Unlimited” systems, Technologies, and Operations. Aerospace, 15-18 September 2003, San Diego, California.

[4] Jean-Luc Boiffier, 1998. *The dynamics of flight, the equations*. John Wiley & Sons, Inc., New York, USA.

[5] PhD thesis, Roberto Naldi, 2008. “Prototyping, Modeling and Control of a Class of VTOL Aerial Robots”. PhD Thesis, University of Bologna, Italy.

[6] Iain K. Peddle, Thomas Jones, Johann Treurnicht, 2008. “Practical near hover flight control of a ducted fan (SLADe)”. *Journal of Control Engineering Practice,* 17, pp. 48-58.

[7] Katsuhiko Ogata, 2002. *Modern Control Engineering*. Prentice Hall, USA.

[8] Tal Shima, Steven Rasmussen, 2009. *UAV Cooperative Decision and Control.* Siam, Philadelphia, USA.